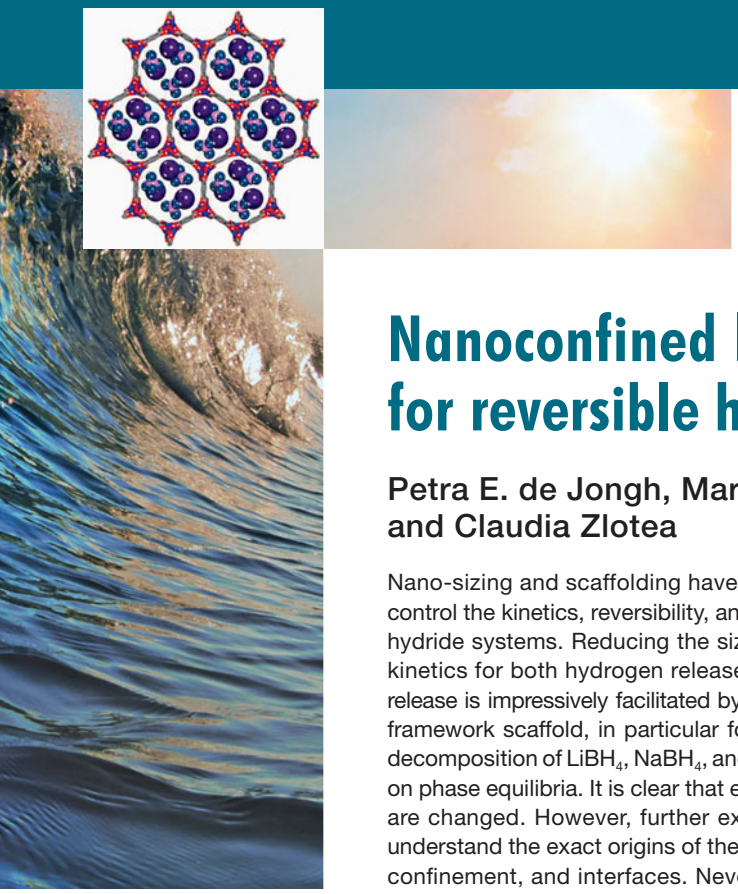


Nanoconfined light metal hydrides for reversible hydrogen storage

Petra E. de Jongh, Mark Allendorf, John J. Vajo, and Claudia Zlotea

Nano-sizing and scaffolding have emerged in the past decade as important strategies to control the kinetics, reversibility, and equilibrium pressure for hydrogen storage in light metal hydride systems. Reducing the size of metal hydrides to the nanometer range allows fast kinetics for both hydrogen release and subsequent uptake. Reversibility of the hydrogen release is impressively facilitated by nanoconfining the materials in a carbon or metal–organic framework scaffold, in particular for reactions involving multiple solid phases, such as the decomposition of $LiBH_4$, $NaBH_4$, and $NaAlH_4$. More complex is the impact of nanoconfinement on phase equilibria. It is clear that equilibrium pressures, and even decomposition pathways, are changed. However, further experimental and computational studies are essential to understand the exact origins of these effects and to unravel the role of particle size, physical confinement, and interfaces. Nevertheless, it has become clear that nanoconfinement is a strong tool to change physicochemical properties of metal hydrides, which might not only be of relevance for hydrogen storage, but also for other applications such as rechargeable batteries.

Introduction

Solid-state systems provide an attractive option for safe and compact hydrogen storage. High volumetric and gravimetric hydrogen densities are realized if hydrogen is allowed to react reversibly with light metals, such as magnesium, to form metal hydrides. However, none of the light metal hydrides meets all practical hydrogen storage requirements, especially with respect to having fast release, full reversibility, and an equilibrium pressure in the desired range. In the past decade, nanosizing metal hydrides using a porous scaffold has emerged as an effective strategy toward meeting these requirements.[1–4] In this article, we give a brief overview of the impact of nanosizing, especially by employing a nanoscaffold, on the hydrogen storage properties of light metal hydrides, highlighting fundamental aspects, giving practical examples, and discussing possible future developments.

Particle size effects

It is well known that the physicochemical properties of materials change if the particle size is reduced to the low nanometers range. A well-known example is gold, which changes from a golden colored inert metal into a red colored, low melting temperature, reactive, and catalytically active material once the particle size is reduced below 10–20 nm.[5]

What can we expect when we decrease the size of metal hydride particles? In nanoparticles, a significant fraction of the atoms are located at the surface, while none of the interior atoms are very far from the surface. This means that we expect very fast kinetics for hydrogen release and uptake, as these are surface-mediated processes and typically involve diffusion through the solid state. Indeed this is generally observed, quite independent of the exact metal hydride system involved.

Importantly, the equilibrium between metal and hydrogen on one side and the metal hydride on the other side changes. For particles 2–20 nm in size, this is mostly related to the significant contribution of the surface energy term to the overall stability of the nanoparticles. If the metal hydride has a much larger surface energy than the metal, the equilibrium will shift toward the metal with decreasing size; however, if the metal has a higher surface energy, the situation is reversed. This is illustrated in **Figure 1**, which depicts the theoretically predicted change in equilibrium hydrogen release temperatures

Petra E. de Jongh, Debye Institute for Nanomaterials Science–Utrecht University, The Netherlands; P.E.deJongh@uu.nl
Mark Allendorf, Sandia National Laboratories, CA, USA; mdallen@sandia.gov
John J. Vajo, HRL Laboratories, CA, USA; JJVajo@hrl.com
Claudia Zlotea, Institut de Chimie et des Materiaux–Paris, France; claudia.zlotea@icmpe.cnrs.fr
DOI: 10.1557/mrs.2013.108

© 2013 Materials Research Society
https://doi.org/10.1557/mrs.2013.108 Published online by Cambridge University Press

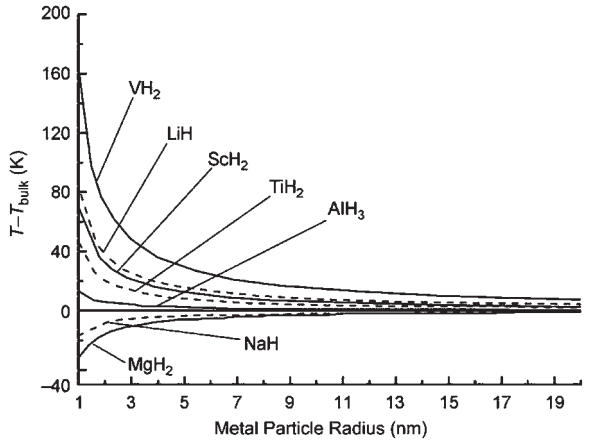


Figure 1. The hydrogen release temperature T for nanometer-sized metal hydride particles is different than the release temperature T_{bulk} for micrometer-sized particles. The figure shows calculated differences for a range of metal hydrides as a function of particle size. Reprinted with permission from Reference 6. © 2009 IOP Publishing.

under 1 bar H_2 pressure as a function of particle size for different metal-metal hydride combinations.[6] For small clusters, even the atomic structure often deviates from the bulk structure, and changes in M–H and H–H interactions can play an important role. Large changes in equilibrium pressure are generally expected only below 2–5 nm particle size.[6–8] One of the earliest systems for which this has been calculated in detail is the MgH_2 system, for which the equilibrium temperature (at 1 bar H_2 pressure) based on the change in enthalpy of reaction is calculated to decrease from ~300°C for µm-sized crystallites to 200°C for 0.9 nm clusters.[7]

Palladium hydride as a model system to study size effects

The metal-hydrogen system for which particle size effects have been studied experimentally in most detail is Pd–H.[9–12] It is not considered to be a practical hydrogen storage system due to its low gravimetric hydrogen content (0.65 wt%) and high cost, but it provides very fast hydrogen release and uptake, and the hydrogen equilibrium pressure at room temperature is close to 1 bar, making it a convenient model system for interstitial metal hydrides.

The equilibrium pressure-composition-isotherms show significant size effects (**Figure 2**a). The allowed hydrogen content in the solid solution phase (α) increases, whereas it decreases in the hydride phase (β) with reducing size. Consequently, the miscibility gap (two-phase region) narrows, and the critical temperature is lower for smaller particles.[10–13] Also, the equilibrium pressure in the two-phase region is not constant, but increases with increasing hydrogen content. The amount of hydrogen stored in the interior of Pd nanoparticles is lower than bulk Pd; however, this can be compensated for by a larger amount of hydrogen bound at surface and subsurface sites.

A plausible explanation is based on thermodynamic changes (enthalpy and entropy of mixing) in nano-sized Pd–H systems. Yamauchi et al. found that the thermodynamic quantities $-\Delta H_{\alpha\rightarrow\beta}$ (enthalpy of hydrogenation) and $-\Delta S_{\alpha\rightarrow\beta}$ (entropy) decrease by reduction of size (Figure 2b).[11] It was argued that the nonconstant equilibrium pressure in the two-phase region is induced by a distribution of size-related surface tensions, interfacial stresses, or due to structural heterogeneities.[10,11]

Confining metal hydride nanoparticles in carbon scaffolds

Small particles are intrinsically unstable and prone to grow into larger crystallites. In suspensions, they can be stabilized by ligands, but in the solid phase, stabilization is typically achieved by placing the nanomaterial inside a porous host (a "support," "scaffold," or "matrix"). In the case of metal hydride storage systems, the host should comply with several requirements, including low weight, low cost, high porosity, and sufficient chemical inertness to limit reaction with the light metals.[13,14] Porous carbon materials, such as carbon aerogels, high surface area graphite, and carbon replicas of ordered mesoporous materials basically satisfy all of these criteria, and hence have overwhelmingly been investigated as the scaffold of choice.[1]

Different methods are used to prepare carbon-confined materials. Two representative resulting carbon-supported metal nanoparticulate samples are shown in **Figure 3**. Solution-impregnation based strategies involve several steps: (1) liquid impregnation of hosts by solutions of either the metal hydrides

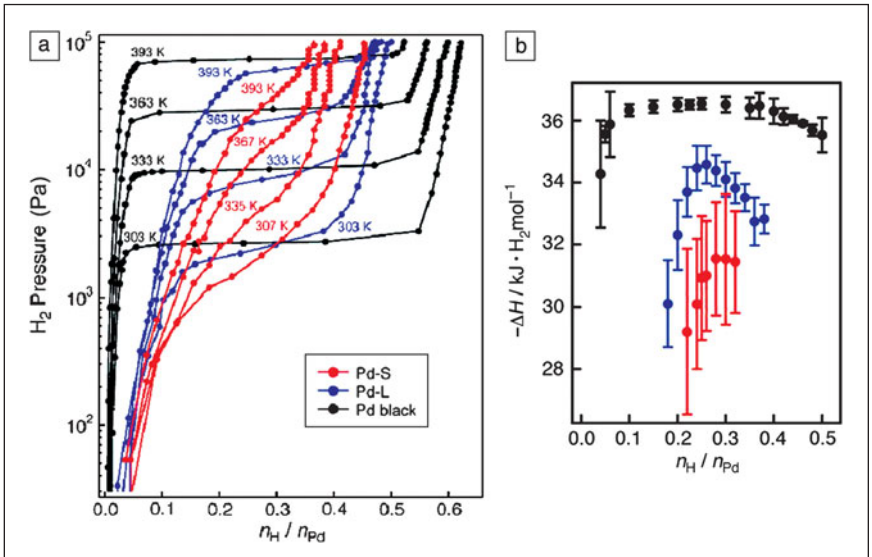


Figure 2. (a) Pressure-composition isotherms at different temperatures (as indicated) for bulk Pd powder (Pd black), 7.0 nm Pd particles (Pd-L), and 2.6 nm Pd particles (Pd-S). (b) Hydrogenation enthalpy derived from the measurements shown in (a). The x-axis (n_H/n_{Pd}) is the ratio of H to Pd. Reprinted with permission from Reference 11. © 2008 American Chemical Society.

https://doi.org/10.1557/mrs.2013.108 Published online by Cambridge University Press

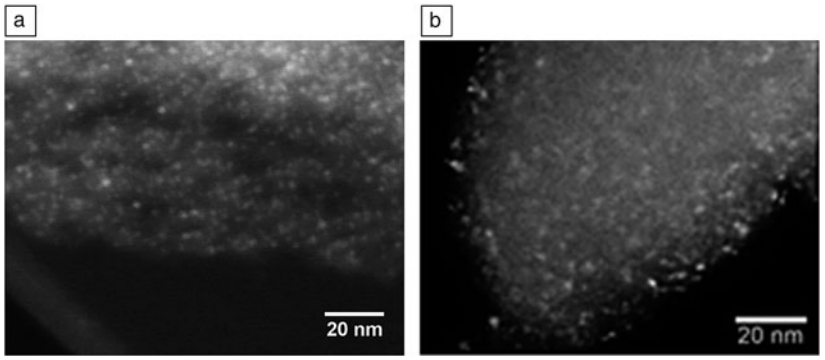


Figure 3. Dark-field electron micrographs (with the metal nanoparticles showing as bright dots) of (a) Pd nanoparticles and (b) Mg nanoparticles, both embedded in mesoporous carbon templates.[12,22]

themselves or precursors (e.g., $NaAlH_4$ or $LiBH_4$ in THF, diethyl- or dibutylmagnesium in diethyl ether, hexane or heptane, palladium chlorides in aqueous solution); (2) if relevant, *in situ* reduction to the corresponding metals or hydrogenation to the respective hydrides (Figure 3a: dark-field TEM image of Pd nanoparticles in a carbon scaffold); and (3) removal of the solvent.[15–21] An alternative synthesis technique is melt infiltration with either the metal itself (Figure 3b: dark-field TEM image of Mg nanoparticles in a carbon scaffold), or the metal hydride ($NaAlH_4$, $LiBH_4$, $NaBH_4$) in an inert or hydrogen atmosphere.[22–28] Complex metal hydrides generally wet carbon matrices well and allow almost complete pore filling. It is more difficult to deposit light metal nanoparticles inside the pores, in some cases vapor phase transport also plays a role, and sometimes transition metals are predeposited to facilitate wetting/nucleation of confined particles.[27,28] Another technique is mechanochemical synthesis via a metathesis reaction. An example is the reaction between LiH and $MgCl_2$, for which the final product is a dispersion of MgH_2 nanoparticles in a LiCl matrix.[29] Simply ball-milling scaffold and metal (hydride) generally destroys porous carbon structures and hence does not result in well-defined nanoconfined materials.

The scaffold is essential to stabilize the nanoparticles and often facilitates their synthesis in the first place. Furthermore, it often has a profound impact on the properties of the confined phases. Physical confinement and chemical bonding between the scaffold and active material can induce mechanical stress and will certainly influence energetics, shape, and size of the active material after preparation but also during hydrogen cycling.[13,14] Whether catalytically active metal nanoparticles such as Pd could significantly increase the hydrogen uptake of high surface area carbon materials at ambient temperature due to spillover remains under discussion.[30]

Nanoconfinement of magnesium hydride to enhance kinetics

Magnesium hydride is the ionic hydride most studied for hydrogen storage. It has an appreciable hydrogen content (7.65 wt%) but slow sorption kinetics and high thermodynamic stability ($\Delta H_f^0 = -75$ kJ mol^{-1} and $\Delta S_f^0 = -135$ J mol^{-1} K^{-1}). Nano-sizing and nanoconfinement of MgH_2 particles significantly improve the hydrogen desorption/absorption kinetics (**Figure 4**a), and faster hydrogen release is observed for smaller pore sizes.[18,20,28,31] Nanoconfinement can be combined with the addition of transition metals to enhance the desorption kinetics even further, as they act as hydrogenation catalysts and alloying elements.[27,28,32] MgH_2 nanoparticles embedded in porous carbon show rather good hydrogen cycling stability. The reversible hydrogen capacity is 5.5–7 wt% for more than 10 cycles (Figure 4b).[18,20]

Significant thermodynamic destabilization has been predicted theoretically for MgH_2 particles of less than 1–2 nm size.[7,8] Experimentally, it is difficult to attain such small particle sizes. MgH_2 nanoparticles (~7 nm) embedded in LiCl show only slight thermodynamic changes ($-\Delta H_f = 71$ kJ mol^{-1} and $-\Delta S_f = 130$ J mol^{-1} K^{-1}).[29] Smaller MgH_2 nanoparticles (~3 nm) in a carbon scaffold show a larger shift in reaction enthalpy ($-\Delta H_f = 63.8$ kJ mol^{-1}), but this is counteracted by a shift in entropy ($-\Delta S_f = 117.2$ J mol^{-1} K^{-1}), hence the equilibrium temperature at 1 bar is only 11°C lower than for bulk MgH_2.[33] However, it should be noted that particle sizes of MgH_2 after cycling are seldomly determined, while severe sintering can occur for Mg nanoparticles during cycling.[32] In general, we can conclude that in the case of MgH_2, the kinetics of hydrogen sorption are greatly enhanced, but only limited thermodynamic destabilization of the hydride may be achieved by nanoconfinement.

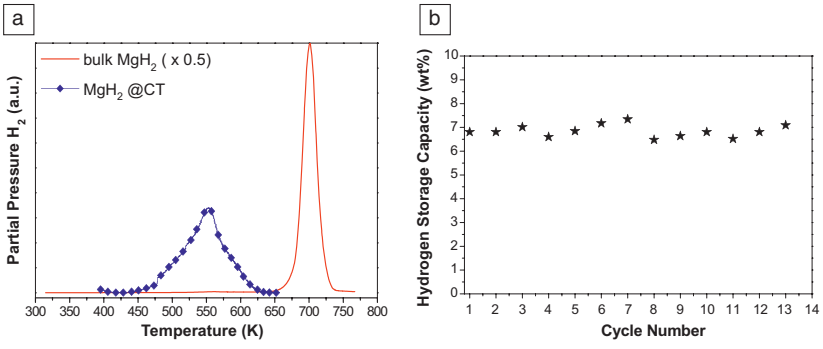


Figure 4. Hydrogen sorption properties for MgH_2 nanoparticles (mean size ~5 nm) embedded into a carbon scaffold (MgH_2@CT). (a) Hydrogen desorption compared with bulk MgH_2 (10°C/min); (b) storage capacity over 13 hydrogen absorption/desorption cycles.[20] Reprinted with permission from Reference 20. © 2011 Royal Society of Chemistry.

https://doi.org/10.1557/mrs.2013.108 Published online by Cambridge University Press

Nanoconfinement of complex metal hydrides

Sodium alanate, $NaAlH_4$, is one of the most studied complex metal hydrides (see the article by Graetz et al. in this issue). It decomposes in several hydrogen release steps via the hexahydride Na_3AlH_6 to NaH, giving a modest hydrogen capacity of 5.6 wt% (or 7.4 wt% if full decomposition to Na, Al, and H_2 is considered). Interestingly, the desorption/absorption equilibriums under 1 bar H_2 pressure are in the desired temperature range for compatibility with proton exchange membrane fuel cells (33°C for $NaAlH_4$ and 110°C for Na_3AlH_6 decomposition), and it is the only complex metal hydride for which an effective catalyst (Ti-based) has been identified.[34]

The advantages of combining carbon supports with $NaAlH_4$ were first mentioned in a patent application in 2004,[35] but the first results in open literature appeared in 2006.[15] Low loadings of $NaAlH_4$ on carbon were prepared by impregnation with $NaAlH_4$ in THF solution. Bulk $NaAlH_4$ without a catalyst only starts to release a significant amount of hydrogen around the melting point of $NaAlH_4$ (~180°C). This essentially prevents reversible hydrogenation of bulk $NaAlH_4$. In contrast, $NaAlH_4$ nanoparticles on carbon nanofibers start to release hydrogen at room temperature, even without a Ti-based catalyst. A strong particle size dependence of the hydrogen release temperature was found, with an activation energy of only 58 kJ mol^{-1} for 2–10 nm particles, while 120 kJ mol^{-1} is reported for bulk $NaAlH_4$, and ~80 kJ mol^{-1} in the presence of a Ti-based catalyst.[36]

Melt infiltration allows high loadings of $NaAlH_4$; it is possible to fill the pores of a carbon host almost completely. Hydrogen release in these highly loaded nanoconfined systems generally occurs at higher temperatures than for supported nanoparticles of similar size, and it does not depend strongly on host pore size.[37] However, very good reversibility (>80–90%) under relatively mild conditions is obtained even without a catalyst, especially if care is taken to compensate or avoid side reactions with the host material.[24,38] The scaffold prevents large-scale phase segregation upon decomposition, and most likely the carbon host surface also provides efficient surface-mediated transport of metal-based species.[38] Furthermore, it has been postulated that carbon materials could act as "catalysts" for dehydrogenation involving electronic effects.[39] Kinetics can be further enhanced by combining nanoconfinement with Ti-based catalysts.[37]

Nanoconfinement clearly changes the phase equilibriums in the Na-Al-H system (**Figure 5**). The two-phase equilibrium results in sloping rather than flat plateaus in the pressure-composition isotherms (Figure 5a).[40] The $NaAlH_4$ phase actually becomes more stable with respect to its decomposition products upon nanoconfinement in carbon hosts, and the formation of the Na_3AlH_6 phase becomes unfavorable (Figure 5b),[41] according to both experimental findings and theoretical calculations.[24,40–43]

A second interesting family of complex metal hydrides is the alkali metal borohydrides. $LiBH_4$ has received much attention, as it contains 18.5 wt% hydrogen. However, the hydride is much more stable than $NaAlH_4$ and also decomposes in several steps, with LiH and $Li_2B_{12}H_{12}$ being reported as very stable phases.[44] However, the most important impediment for practical use is the limited reversibility, which is most likely related to the inert boron phase being formed upon dehydrogenation. For bulk $LiBH_4$, partial reversibility has been reported only at 600°C and 155 bar H_2 pressure.

$LiBH_4$ can be deposited in porous hosts from solution,[16] but almost full pore filling is conveniently obtained by melt infiltration, as first reported by Gross et al.[23] Again, hydrogen release kinetics are largely improved by nanoconfinement in carbon (**Figure 6**a). This improvement might be related to increased ionic mobilities at low temperatures for $LiBH_4$ confined in nanoporous hosts, as evident from nuclear magnetic

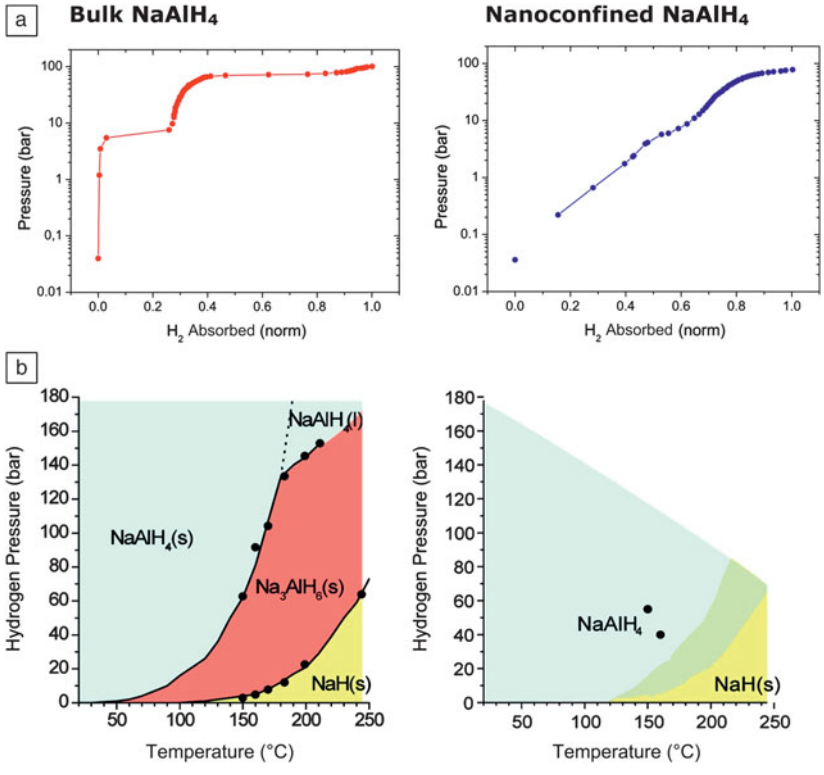


Figure 5. Equilibria for the Na-Al-H system, comparing bulk $NaAlH_4$ (left frames) to carbon nanoconfined $NaAlH_4$ (right frames). (a) Pressure composition isotherms, with two clear decomposition steps (forming first Na_3AlH_6 and then NaH and Al) for the bulk, while for the nanoconfined sample, a rather continuous hydrogen release is observed (figures courtesy of M. Fichtner).[40] (b) Bulk phase diagram showing three clearly defined phase regions. For the nanoconfined sample, an indicative phase diagram is shown, with the markers representing conditions for which the presence of $NaAlH_4$ and the absence of Na_3AlH_6 were confirmed by solid-state nuclear magnetic resonance. Reprinted with permission from Reference 41. © 2010 American Chemical Society.

https://doi.org/10.1557/mrs.2013.108 Published online by Cambridge University Press

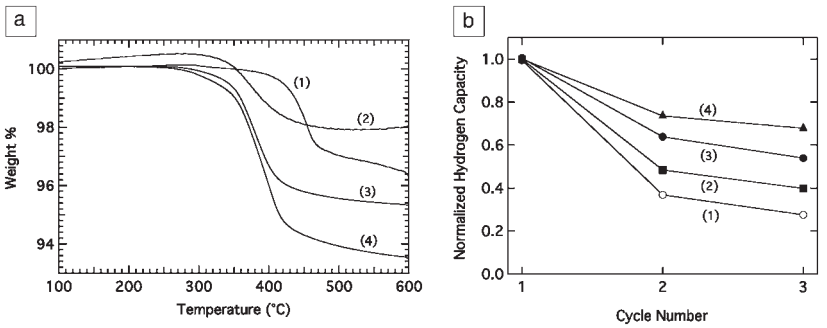


Figure 6. (a) Normalized hydrogen desorption and (b) cycling stability for $LiBH_4$ incorporated in carbon scaffolds. Curve (1) $LiBH_4$ mixed with nonporous graphite. Curve (2) $LiBH_4$ incorporated into activated carbon. Curve (3) $LiBH_4$ incorporated into 13 nm carbon aerogel. Curve (4) $LiBH_4$ incorporated into 25 nm carbon aerogel. Reprinted with permission from Reference 23. © 2008 American Chemical Society.

resonance measurements.[45,46] The improvement in reversibility under mild conditions is spectacular (Figure 6b),[23] especially if Ni is added.[47] This is mostly attributed to physical confinement, keeping the phases small and with large interfacial areas during hydrogen cycling. However, suppression of the formation of gaseous decomposition products other than H_2 also seems to play a role.[16,48]

In some cases, specific interactions with the carbon host are observed. An interesting possibility is the formation of lithium-doped fullerenes (Li_x-$C_{60}H_y$) that are capable of reversibly storing 5 wt% hydrogen.[49] Furthermore, reversible intercalation of Na into the carbon can occur, stabilizing the metal phase and lowering the equilibrium decomposition temperature of NaH under 1 bar H_2 pressure from 425°C to 225°C.[50]

Recent developments beyond carbon scaffolds

The carbon hosts discussed until now are rather heterogeneous materials, and it would be desirable to attain smaller (<1–2 nm) metal (hydride) particles. Metal–organic frameworks (MOF) are attractive scaffolds in this respect, because their crystalline structure yields highly defined, monodisperse micropores (<2 nm). Since systematic tuning of both pore size and chemical environment is feasible,[51] the potential exists to isolate the effects of particle size from surface chemistry to a great extent.

Wet-chemical methods have been used to deposit Pd in MOF, showing a synergistic effect of hydrogen physisorption by the porous MOF, hydrogen uptake by the Pd, and possibly a contribution from spillover. However, the effective hydrogen uptake at room temperature is limited (~0.35 wt%).[52] In a recent study, Lim et al. formed Mg nanocrystals by thermally decomposing bis-cyclopentadienyl magnesium ($MgCp_2$) after exposing a MOF to vapors of this organometallic compound. The resulting hybrid material exhibits synergistic behavior in which the heat of H_2 physisorption increases to as much as 11.6 kJ mol^{-1}, while simultaneously, the release temperature for chemisorbed hydrogen decreases by >200 K relative to 50–100 μm Mg powder.[53]

Bhakta et al. were the first to demonstrate that the 1.3 nm pore MOF $Cu_3(BTC)_2$ (benzenetricarboxylate) can be infiltrated with $NaAlH_4$ from a THF solution without framework degradation, forming clusters with only eight formula units on average.[17] The reaction to NaH, Al, and H_2 proceeds by a single step, and H_2 desorption is dramatically accelerated (the desorption activation energy is reduced by more than 60 kJ $(mol\text{-}H_2)^{-1}$) relative to the bulk.[54] This acceleration of desorption kinetics is observed across a range of metal hydrides. In the case of $LiBH_4$ synthesized by confinement within the pores of Cu-containing MOFs, the enhanced hydrogen desorption rates are thought to result from interactions between the hydride and open coordination sites on the Cu(II) ions in the framework.[55]

Reactions between confined metal (hydride) clusters and the metal–organic framework can be an issue. Recently, reversible cycling of nanoconfined $NaAlH_4$ was reported (**Figure 7**).[54,56] Bhakta et al. achieved reversible cycling with only a modest reduction in capacity from 4.1 wt% to 3.6 wt% over four cycles by melt infiltrating $NaAlH_4$ into a titanium-modified MOF.[54] This suggests that the open coordination sites stabilize the catalyst, and the pore dimensions are sufficiently small to prevent agglomeration of product phases. Hopefully, the achievement of confining metal hydrides in porous MOFs and hydrogen cycling them without structural degradation will open new possibilities to gain a more fundamental understanding of particle size effects.

All scaffold materials discussed so far decrease the overall hydrogen capacity of the systems significantly by their added

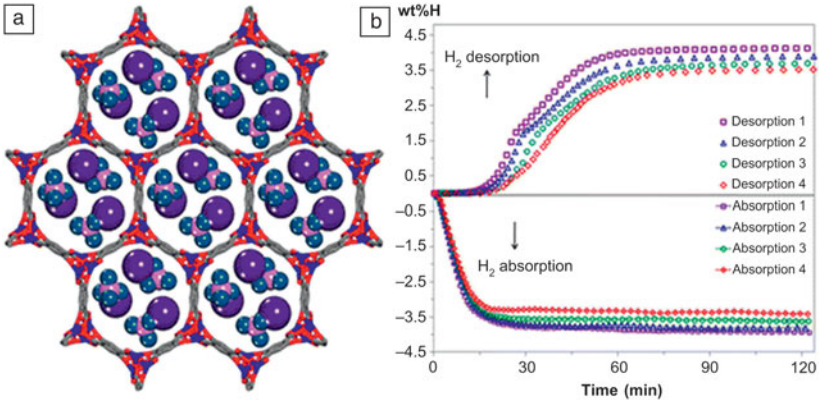


Figure 7. $NaAlH_4$ confined in the nanopores of a titanium-functionalized metal–organic framework MOF-74 (Mg) forms clusters of formula units (a) and can reversibly store hydrogen with minimal loss of capacity. (b) wt% normalized to the $NaAlH_4$ loading. Reprinted with permission from Reference 56. © 2012 American Chemical Society.

https://doi.org/10.1557/mrs.2013.108 Published online by Cambridge University Press

weight. Furthermore, nano-sizing metal particles enhances not only the kinetics of hydrogenation, but also the risk of oxidation (and hence passivation) as well as evaporation. As an alternative approach, air-stable Mg nanoparticles (~5 nm) embedded in a hydrogen gas-selective polymer matrix (PMMA) were recently described, prepared by a one-pot reduction of an Mg organometallic precursor. The Mg nanoparticles (~5 nm) incorporated in a polymer absorb hydrogen relatively fast at 35 bar and 200°C (6 wt% in 60 min).[57] Another intriguing option is a core-shell system. $NaBH_4$ particles individually encapsulated in catalytically active Ni shells give hydrogen release rates and reversibilities unprecedented for $NaBH_4$.[58]

An open question is whether the changes in properties observed due to nanoconfinement might also be relevant for other applications. For instance, $LiBH_4$ is proposed as a possible solid Li^+ conductor for rechargeable lithium batteries. Generally, the hydrogen and lithium mobilities below the solid-solid phase transition temperature (110°C) are low. However, greatly enhanced hydrogen dynamics and lithium translational mobility are observed if the $LiBH_4$ is confined in the nanopores of a carbon or silica matrix.[45,46]

Conclusion and outlook

In the past decade, confining metal hydrides inside nanopores has emerged as an intriguing strategy to influence the material characteristics that are essential for reversible hydrogen storage. Hydrogen release temperatures are lowered substantially by nano-sizing, and reversibility under mild conditions is often obtained, even for alkali metal borohydrides, which are notoriously difficult to hydrogen cycle. The strategy is also associated with disadvantages, most notably a lower gravimetric system hydrogen capacity and an increased sensitivity toward passivation by oxidation.

It is clear that particle size, physical confinement, and interfaces are important tools to change the functional characteristics of light metal hydrides. We have just started to explore and unravel the physical origin of the impact of nanoconfinement on fundamental physical-chemical properties. Nevertheless, the improvement in practical performance that has been achieved in such a short time span is impressive and holds great promise for future developments.

Acknowledgments

J.J.V. acknowledges support by the US Department of Energy (DOE contract DEE-FC36–05G015067). P.E.dJ acknowledges financial support from NWO-Vidi and NWO-ACTS/Sustainable Hydrogen.

References

1. P.E. de Jongh, P. Adelhelm, *ChemSusChem* **3**, 1332 (2010).
2. M. Fichtner, *PCCP* **13**, 21186 (2011).
3. T.K. Nielsen, F. Besenbacher, T.R. Jensen, *Nanoscale* **3**, 2086 (2011).
4. J.J. Vajo, *Curr. Opin. Solid State Mater. Sci.* **15**, 52 (2012).
5. E. Roduner, *Chem. Soc. Rev.* **35**, 583 (2006).
6. K.C. Kim, B. Dai, J.K. Johnson, D.S. Sholl, *Nanotechnology* **20**, 204001 (2009).
7. R.W.P. Wagemans, J.H. van Lenthe, P.E. de Jongh, A.J. van Dillen, K.P. de Jong, *J. Am. Chem. Soc.* **127**, 16675 (2005).
8. S. Cheung, W.Q. Deng, A.C.T. van Duin, W.A. Goddard, *J. Phys. Chem. A* **109**, 851 (2005).
9. W.A. Oates, *J. Less-Common Met.* **88**, 411 (1982).
10. A. Pundt, R. Kirchheim, *Ann. Rev. Mater. Res.* **36**, 555 (2006).
11. M. Yamauchi, R. Ikeda, H. Kitagawa, M. Takata, *J. Phys. Chem. C* **112**, 3294 (2008).
12. C. Zlotea, F. Cuevas, V. Paul-Boncour, E. Leroy, P. Dibandjo, R. Gadiou, C. Vix-Guterl, M. Latroche, *J. Am. Chem. Soc.* **132**, 7720 (2010).
13. C. Wu, H.-M. Cheung, *J. Mater. Chem.* **20**, 5390 (2010).
14. P. Adelhelm, P.E. de Jongh, *J. Mater. Chem.* **21**, 2417 (2011).
15. C.P. Baldé, B.P.C. Hereijgers, J.H. Bitter, K.P. de Jong, *Angew. Chem. Int. Ed.* **45**, 3501 (2006).
16. S. Cahen, J.B. Eymery, R. Janot, J.-M. Tarascon, *J. Power Sources* **189**, 902 (2009).
17. R.K. Bhakta, J.L. Herberg, B. Jacobs, A. Highley, R. Behrens, N.W.G. Ockwig, M.D. Allendorf, *J. Am. Chem. Soc.* **131**, 13198 (2009).
18. S. Zhang, A.F. Gross, S.L. van Atta, M. Lopez, P. Liu, C.C. Ahn, J.J. Vajo, C.M. Jensen, *Nanotechnology* **20**, 204027 (2009).
19. T.K. Nielsen, K. Manickam, M. Hirscher, F. Besenbacher, T.R. Jensen, *ACS Nano* **3**, 3521 (2009).
20. C. Zlotea, C. Chevalier-Cesar, E. Leonel, E. Leroy, F. Cuevas, P. Dibandjo, C. Vix-Guterl, T. Martens, M. Latroche, *Faraday Discuss.* **151**, 117 (2011).
21. S. Zheng, F. Fang, G. Zhou, G. Chen, L. Ouyang, M. Zhu, D. Sun, *Chem. Mater.* **20**, 3954 (2008).
22. P.E. de Jongh, R.W.P. Wagemans, T.M. Eggenhuisen, B.S. Dauvillier, P.B. Radstake, J.D. Meeldijk, J.W. Geus, K.P. de Jong.,*Chem. Mater.* **19**, 6052 (2007).
23. A.F. Gross, J.J. Vajo. S.L. van Atta, G.L. Olson, *J. Phys. Chem. C* **112**, 5651 (2008).
24. R.D. Stephens, A.F. Gross, S.L. van Atta, J.J. Vajo, F.E. Pinkerton, *Nanotechnology* **20**, 204018 (2009).
25. P. Adelhelm, J. Gao, M.H.W. Verkuijlen, C. Rongeat, M. Herrich, P.J.M. van Bentum, O. Gutfleisch, A.P.M. Kentgens, K.P. de Jong, P.E. de Jongh, *Chem. Mater.* **22**, 2233 (2010).
26. T.K. Nielsen, M. Polanski, D. Zasada, P. Javadian, F. Besenbacher, J. Bystrzycki, J. Skibsted, T.R. Jensen, *ACS Nano* **5**, 4056 (2011).
27. A.F. Gross, C.C. Ahn, S.L. Van Atta, P. Liu, J.J. Vajo, *Nanotechnology* **20**, 204005 (2009).
28. R. Bogerd, P. Adelhelm, J.H. Meeldijk, K.P. de Jong, P.E. de Jongh, *Nanotechnology* **20**, 204019 (2009).
29. M. Paskevicius, D.A. Sheppard, C.E. Buckley, *J. Am. Chem. Soc.* **132**, 5077 (2010).
30. G.M. Psofogiannakis, G.E. Froudakis, *Chem. Commun.* **47**, 7933 (2011).
31. M. Konarova, A. Tanksale, J. Norberto Beltramini, G. Qing Lu, *Nano Energy* **2**, 12 (2012).
32. Z. Zhao-Karger, J.J. Hu, A. Roth, D. Wang, C. Kubel, W. Lohstroh, M. Fichtner, *Chem. Commun.* **46**, 8353 (2010).
33. C. Zlotea, F. Cuevas, J. Andrieux, C.M. Ghimbeu, E. Leroy, E. Léonel, S. Sengmany, C.V. Guterl, R. Gadiou, T. Martens, M. Latroche, *Nano Energy* **2**, 12 (2012).
34. B. Bogdanović, M. Schwickardi, *J. Alloys Comp.* **253–254**, 1 (1997).
35. F. Schüth, B. Bogdanović, B. Taguchi, US Patent W02005/014469 (2003).
36. C.P. Baldé, B.P.C. Hereijgers, J.H. Bitter, K.P. de Jong, *J. Am. Chem. Soc.* **130**, 6761 (2008).
37. T.K. Nielsen, P. Javadian, M. Polanski, F. Besenbacher, J. Bystrzycki, T.R. Jensen, *J. Phys. Chem. C* **116**, 21046 (2012).
38. J. Gao, P. Ngene, I. Lindemann, O. Gutfleisch, K.P. de Jong, P.E. de Jongh, *J. Mater. Chem.* **22**, 13209 (2012).
39. P. Berseth, A.G. Harter, R. Zidan, A. Blomqvist, C. Moyses Araujo, R.H. Scheicher, R. Ahuja, P. Jena, *Nano Lett.* **9**, 1501 (2009).
40. W. Lohstroh, A. Roth, H. Hahn, M. Fichtner, *ChemPhysChem* **11**, 789 (2010).
41. J. Gao, P. Adelhelm, M.H.W. Verkuijlen, C. Rongeat, M. Herrich, P.J.M. van Bentum, O. Gutfleisch, A.P.M. Kentgens, K.P. de Jong, P.E. de Jongh, *J. Phys. Chem. C* **114**, 4674 (2010).
42. T. Mueller, G. Ceder, *ACS Nano* **4**, 5647 (2010).
43. E.H. Majzoub, F. Zhou, V. Ozoliņš, *J. Phys. Chem. C* **115**, 2636 (2011).
44. S. Orimo, Y. Nakamori, G. Kitagawa, K. Miwa, N. Ohba, S. Towatat, A. Züttel, *J. Alloys Comp.* **404**, 427 (2005).
45. D.T. Shane, R.L. Corey, C. McIntosh, L.H. Rayhel, R.C. Bowman Jr., J.J. Vajo, A.F. Gross, M.S. Conradi, *J. Phys. Chem. C* **114**, 4008 (2010).
46. M.H.W. Verkuijlen, P. Ngene, D.W. de Kort, C. Barre, A. Nale, E.R.H. van Eck, P.J.M. van Bentum, P.E. de Jongh, A.P.M. Kentgens, *J. Phys. Chem. C.* **116**, 22169 (2012).
47. P. Ngene, M.H.W. Verkuijlen, Q. Zheng, J. Kragten, P.J.M. van Bentum, J.H. Bitter, P.E. de Jongh, *Faraday Discuss.* **151**, 47 (2011).

https://doi.org/10.1557/mrs.2013.108 Published online by Cambridge University Press

48. X. Liu, D. Peaslee, C.Z. Jost, T.F. Baumann, E.H. Majzoub, *Chem. Mater.* **23**, 1331 (2011).
49. J.A. Teprovich Jr, M.S. Wellons, R. Lascola, S.-J. Hwang, P.A. Ward, R.N. Compton, R. Zidan, *Nano Lett.* **12**, 582 (2012).
50. P. Adelhelm, K.P. de Jong, P.E. de Jongh, *Chem. Commun.* **41**, 6261 (2009).
51. G. Ferey, *Chem. Soc. Rev.* **37**, 191 (2008).
52. C. Zlotea, R. Campesi, F. Cuevas, E. Leroy, P. Dibandjo, C. Volkringer, T. Loiseau, G. Ferey, M. Latroche, *J. Am. Chem. Soc.* **132**, 2991 (2010).
53. D.-W. Lim, J.W. Roon, K.Y. Ryu, M.P. Suh, *Angew. Chem. Int. Ed.* **51**, 9814 (2012).
54. R.K. Bhakta, S. Maharrey, V. Stavila, A. Highley, T. Alam, E. Majzoub, M. Allendorf, *PCCP* **14**, 8160 (2012).
55. W.W. Sun, S. Li, J. Mao, Z. Guo, H. Liu, S. Dou, X. Yu, *Dalton Trans.* **40**, 5673 (2011).
56. V. Stavila, R.K. Bhakta, T.M. Alam, E.H. Majzoub, M.D. Allendorf, *ACS Nano* (2012); doi:10.1021/nn304514c.
57. K.J. Jeon, H.R. Moon, A.M. Ruminski, B. Jiang, C. Kisielowski, R. Bardhan, J.J. Urban, *Nat. Mater.* **10**, 286 (2011).
58. M.L. Christian, K.-F. Aguey-Zinsou, *ACS Nano* **6**, 7739 (2012). □

MRS ENERGY & SUSTAINABILITY
A Review Journal

EDITORS-IN-CHIEF
David S. Ginley, National Renewable Energy Laboratory
David Cahen, Weizmann Institute of Science
Sally M. Benson, Stanford University

Coming Early 2014

MRS Energy & Sustainability: A Review Journal will publish reviews on key topics in materials research and development as they relate to energy and sustainability. Topics to be reviewed include new R&D of both established and new areas; interdisciplinary systems integration; and objective application of economic, sociological, and governmental models, enabling research and technological developments. The reviews will be set in an integrated context of scientific, technological and sociological complexities relating to environment and sustainability.

The intended readership is a broad spectrum of scientists, academics, policy makers and industry professionals, all interested in the interdisciplinary nature of the science, technology and policy aspects of energy and sustainability.

For more information, including author benefits, open access options, indexing and proposal form, visit **www.mrs.org/energy-sustainability-journal.**

MRS MATERIALS RESEARCH SOCIETY® Advancing materials. Improving the quality of life.
CAMBRIDGE UNIVERSITY PRESS

SONICATOR Ultrasonic Liquid Processors



High-powered nanoparticle dispersion systems

- **disperse**
- **deagglomerate**
- **reduce particle size**

Probe sonication is highly effective for processing nanomaterials (carbon nanotubes, graphene, inks, metal oxides, etc.). Contact us to have a product specialist review your application.



Qsonica has manufactured ultrasonic equipment for over 40 years. Our products are made in the USA and include a 2-year warranty.

QSONICA SONICATORS

Phone: 203.426.0101 • www.sonicator.com/nano

https://doi.org/10.1557/mrs.2013.108 Published online by Cambridge University Press